



# Synthesis and self-assembly of a neoglycopeptide: morphological studies and ultrasound-mediated DNA encapsulation<sup>‡</sup>

Nidhi Gour,<sup>§</sup> Sudipta Mondal and Sandeep Verma\*

Self-assembly in peptides and proteins is an often encountered concept, where constituent building blocks are recruited and stabilized, via carefully orchestrated hydrophobic interactions, hydrogen bonding and other non-covalent interactions, to eventually reveal an array of supramolecular aggregates, with defined structural features. This study presents synthesis and self-assembly of a mannosylated peptide in aqueous medium. Turbidimetric assay with Concanavalin A (Con A), a mannose binding protein, was conducted to confirm the presence of hydrophilic mannose group on the exterior surface of self-assembled structures. DNA encapsulation in these soft structures was achieved by ultrasonication of soft spherical structures in the presence of plasmid DNA. Copyright © 2010 European Peptide Society and John Wiley & Sons, Ltd.

Supporting information may be found in the online version of this article

**Keywords:** peptide; self-assembly; vesicles; nanocontainer; DNA encapsulation

## Introduction

Construction of supramolecular architectures, involving self-association or self-assembly of bioessential components such as peptides, offers numerous advantages in terms of material and biochemical applications. Amongst the various possible morphologies achieved with peptide building blocks, the formation of spherical morphology evinces keen interest due to potential scope for guest encapsulation and subsequent application as delivery vehicles [1–4]. In addition, modulated response of soft molecular ensembles to external stimulus further increases their scope as drug delivery systems, (bio)chemical sensors, and cell adhesion mediators, to name a few [5–10]. Modifiable external stimuli of temperature, pH, light, electric field, chemicals and ionic strength, could produce measurable changes in responsive soft matter leading to modified shape and surface properties, solubility characteristics, ability to self-assemble or disassemble [11–17]. As a specific recent example, chemical modification of soft vesicular structures with carbohydrate appendages has been shown to be very useful, resulting in specific and desirable interactions [18].

We have explored the design and synthesis of a small peptide motif to generate desired morphological features with the aim of manipulating them with a suitable and biologically relevant tuning mechanism [19–22]. As a result of our investigations, we have discovered peptide-based supramolecular ensembles which respond to colchicines [23], physiologically relevant cations [24], covalently attached structure modifiers [25,26], and sunlight [27]. In this study, the self-assembly property of the glycopeptide *N*<sup>2</sup>,*N*<sup>6</sup>-bis[( $\alpha$ -D-mannopyranosyl)thio]propionyl]-Lys-Pro-Phe-Phe-Pro-OH studied in aqueous solution and the formation of spherical morphology was confirmed using various microscopic techniques. As an interesting application, we show that these structures can possibly encapsulate plasmid DNA subsequent to mild ultrasonication treatment.

## Materials and Methods

### General

Dichloromethane, *N,N*-dimethylformamide, triethylamine and methanol were distilled, following standard procedures prior to use. DCC, *t*-butyloxycarbonyl carbonate, boron trifluoride etherate, 3-mercaptopropionic acid and L-amino acids were purchased from Spectrochem Pvt. Ltd.; mannose was obtained from SISCO Research laboratories Pvt. Ltd.; perchloric acid, acetic anhydride and acetic acid were purchased from S.d. Fine-chem limited, Mumbai and used without further purification. Concanavalin A (Con A) was purchased from Sigma Aldrich; pBR322 DNA was purchased from Bangalore Genei, India. <sup>1</sup>H and <sup>13</sup>C NMR spectra were recorded on JEOL-JNM LAMBDA 400 model operating at 400 and 100 MHz, respectively and JEOL ECX-500 model operating at 500 and 125 MHz, respectively. HRMS mass spectra were recorded at IIT Kanpur, India, on Waters, Q-ToF Premier Micromass HAB 213 mass spectrometer using capillary voltage of 2.6–3.2 kV.

\* Correspondence to: Sandeep Verma, Department of Chemistry, Indian Institute of Technology Kanpur, Kanpur, 208 016 UP, India. E-mail: sverma@iitk.ac.in

Department of Chemistry, Indian Institute of Technology Kanpur, Kanpur, 208 016 UP, India

‡ Special issue devoted to the E-MRS Symposium C "Peptide-based materials: from nanostructures to applications", 7–11 June 2010, Strasbourg, France.

§ Department of Chemical Sciences, Tata Institute of Fundamental Research, Homi Bhabha Road, Mumbai 400005, India.

## Synthesis and Characterization

### *N*<sup>2</sup>,*N*<sup>6</sup>-Bis[(2, 3, 4, 6-tetra-*O*-acetyl- $\alpha$ -*D*-mannopyranosyl) thio] propionyl]-lysine *N*-hydroxysuccinimide ester

*N*-hydroxysuccinimide (0.13 g, 1.13 mmol) and compound **1** [20] (1.0 g, 1.01 mmol), were taken in a two-necked round bottom flask and dissolved in dry dichloromethane (20 ml). This resulting solution was stirred in ice-cold water under nitrogen atmosphere for 10 min. DCC (0.25 g, 1.2 mmol) was dissolved in dry dichloromethane (5 ml) and added to the reaction mixture in small batches. The stirring was continued for 1 h in ice-cold water followed at room temperature over night. The white precipitate of *N,N*-dicyclohexylurea was filtered off and the filtrate was washed with 10% sodium-bicarbonate solution (2  $\times$  10 ml) and brine solution (2  $\times$  10 ml). The combined organic layer was dried over anhydrous sodium sulfate, followed by the removal of the solvent by evaporation to yield product (0.56 g, 52%).  $R_f = 0.45$  (10% methanol/dichloromethane). The product was used without further purification in next step.

### *N*<sup>2</sup>,*N*<sup>6</sup>-Bis[(2, 3, 4, 6-tetra-*O*-acetyl- $\alpha$ -*D*-mannopyranosyl) thio] propionyl]-Lys-Pro-Phe-Phe-Pro-OMe (**2**)

A solution of *N*-hydroxysuccinimide ester of **1** (0.5 g, 0.46 mmol) in dry dichloromethane (~15 ml) was added to TFA salt of H-Pro-Phe-Phe-Pro-OMe [21] (0.22 g, 0.34 mmol) dissolved in dry DMF (~5 ml) and stirred. TEA (78  $\mu$ l, 0.56 mM) was added to the reaction mixture in a dropwise fashion and the resulting solution was stirred for ~12 h under nitrogen atmosphere. The reaction mixture was evaporated to dryness and the residue obtained was dissolved in dichloromethane (15 ml) and the organic layer was washed with 1 N HCl (2  $\times$  10 ml) and saturated sodium-bicarbonate solution (2  $\times$  10 ml). The combined organic layer was dried over anhydrous sodium sulfate and the solvent was evaporated to yield a yellow oil which was purified using silica gel column chromatography (5–6% CH<sub>3</sub>OH gradient in CH<sub>2</sub>Cl<sub>2</sub>) to give final product as hygroscopic solid (0.28 g, 40.7%).  $R_f = 0.3$  (5% methanol/dichloromethane). <sup>1</sup>H NMR (500 MHz, CDCl<sub>3</sub>, 25 °C, TMS)  $\delta$  (ppm) 1.29–1.36 (q, 2H,  $J = 12.25$  Hz, 24.25 Hz), 1.57–1.60 (d, 2H,  $J = 12.65$ ), 1.70–1.73 (d, 6H,  $J = 13.00$ ), 1.90–2.15 (m, 28H), 2.49–2.57 (m, 2H), 2.89–2.94 (m, 6H), 3.22–3.26 (m, 2H), 3.46–3.46 (m, 6H), 3.64–3.67 (m, 2H), 3.72 (s, 3H), 4.06–4.12 (m, 3H), 4.29–4.32 (m, 7H), 5.17–5.22 (m, 2H), 5.29 (bs, 7H), 6.94–6.96 (m, 2H), 7.13–7.25 (m, 10H), 8.10–8.11 (m, 2H); <sup>13</sup>C NMR (125 MHz, CDCl<sub>3</sub>, 25 °C, TMS)  $\delta$  (ppm) 15.09, 20.40, 20.88, 21.06, 24.61, 25.30, 29.79, 33.07, 50.15, 52.35, 62.52, 65.89, 66.32, 69.17, 69.61, 126.67, 126.80, 128.46, 129.75, 169.83, 170.00, and 171.00.  $m/z$  (HRMS) Calculated [M+Na<sup>+</sup>] 1507.5400, Found 1507.5249.

### *N*<sup>2</sup>,*N*<sup>6</sup>-Bis[( $\alpha$ -*D*-mannopyranosyl)thio]propionyl]-Lys-Pro-Phe-Phe-Pro-OH (**3**)

To a solution of compound **2** (0.2 g, 0.13 mmol) in methanol (10 ml) sodium methoxide (0.09 g, 1.6 mmol) was added and the reaction mixture was stirred for 1 h at room temperature under nitrogen atmosphere. The resulting solution was neutralized on a Amberlite resin column, which was activated prior to use by 2 N HCl, followed by solvent evaporation to yield deprotected compound **2a**. It was further dissolved in minimum volume of methanol and 0.14 ml 1 N NaOH was added. The resulting solution was stirred for 12 h, followed by neutralization by activated Amberlite resin. The deprotected compound **3** was obtained upon solvent

evaporation as hygroscopic solid (0.04 g, 26%).  $R_f = 0.1$  (30% methanol/dichloromethane).  $[\alpha]_D^{25} = +198.5^\circ$  (c 0.2, CH<sub>3</sub>OH); <sup>1</sup>H NMR (500 MHz, DMSO-*d*<sup>6</sup>, 25 °C, TMS)  $\delta$  (ppm) 1.19–1.27 (m, 3H), 1.47–1.84 (m, 13H), 2.08–2.11 (m, 2H), 2.35–2.43 (m, 5H), 2.71–2.77 (m, 10H), 2.99(bs, 6H), 3.57–3.69 (m, 13H), 4.21–4.26, 4.36, 4.44, 4.60–4.69, 4.80, 4.96 (m, 3H), 5.12–5.14 (bs, 2H), 5.56–5.58 (d,  $J = 8.05$  Hz, 2H), 7.11–7.30 (m, 10H), 7.76–7.89 (m, 2H), 8.08–8.12 (m, 2H); <sup>13</sup>C NMR (125 MHz, DMSO-*d*<sup>6</sup>, 25 °C, TMS)  $\delta$  (ppm) 23.41, 24.99, 25.83, 27.24, 27.49, 29.15, 29.47, 31.41, 33.85, 36.27, 37.34, 38.51, 39.59, 39.92, 40.24, 46.90, 47.30, 48.03, 49.12, 52.39, 59.16, 59.87, 61.69, 67.75, 72.03, 72.32, 74.82, 85.70, 126.78, 128.46, 129.91, 157.21, 169.71, 171.07, and 173.69;  $m/z$  (HRMS) Calculated [M+Na<sup>+</sup>] 1157.4399, Found 1157.4395.

## Atomic Force Microscopy

Atomic force microscopy (AFM) was carried out in air using an Agilent Technologies AFM (5500 AFM/SPM) operating under the Acoustic AC mode (AAC). The sample was mounted on the XY stage of the AFM and the integral video camera (NAVITAR, Model N9451A-USO6310233 with the Fiber-light source, MI-150 high intensity illuminator from Dolan-Jenner Industries) was used to locate the regions of interest. Silicon nitride cantilevers with resonant frequency of 150 kHz were used. The average dimension thickness, width and length of cantilever were approximately 2.0, 51 and 446  $\mu$ m, respectively. The scanner model N9524A-USO7480132.xml/N9520A-USO7480152.xml was calibrated and used for imaging. The images were taken in air at room temperature, with the scan speed of 1.5–2.2 lines/s. Data acquisition and analysis were carried out using PicoView<sup>®</sup> 1.4 and Pico Image<sup>®</sup> Basic software, respectively. Fresh solutions of **3** (1 mM) in water were prepared and incubated at 37 °C for 12 h, prior to microscopic investigation. A 10  $\mu$ l aliquot of the solution was transferred onto freshly cleaved mica surface. The sample-coated mica was dried for 30 min under lamp, and finally vacuum was applied for 30 min followed by AFM imaging.

## Scanning Electron Microscopy

A 20  $\mu$ l aliquot of **3** dissolved in water (1 mM) and incubated at 37 °C for 12 h was dried under lamp on copper stubs and subsequently coated with gold. Scanning electron microscopic images were acquired on FEI QUANTA 200 microscope, equipped with a tungsten filament gun, operating at WD 10.6 mm and 20 kV.

## Optical Microscopy

A 20  $\mu$ l aliquot of the **3** (1 mM) dissolved in water and incubated at 37 °C for 16 h was dried under lamp on glass slide and visualized without filter in (Leica DM2500M) microscope under 100 $\times$  lens.

## Fluorescence Microscopy

Compound **3** was dissolved in rhodamine B aqueous solution (1  $\mu$ M) to a final concentration of 1.0 mM and incubated for 16 h at 37 °C. After 16 h, 20  $\mu$ l of the solution was loaded on the glass slide and dried under lamp. Dye stained structures were examined under a fluorescent microscope (Leica DM2500M), provisioned with a rhodamine filter (absorption 540 nm/emission 625 nm). This filter allows optimized visualization of rhodamine-treated (positive resolution) compared with untreated (negative resolution) vesicles that are virtually invisible to this light.

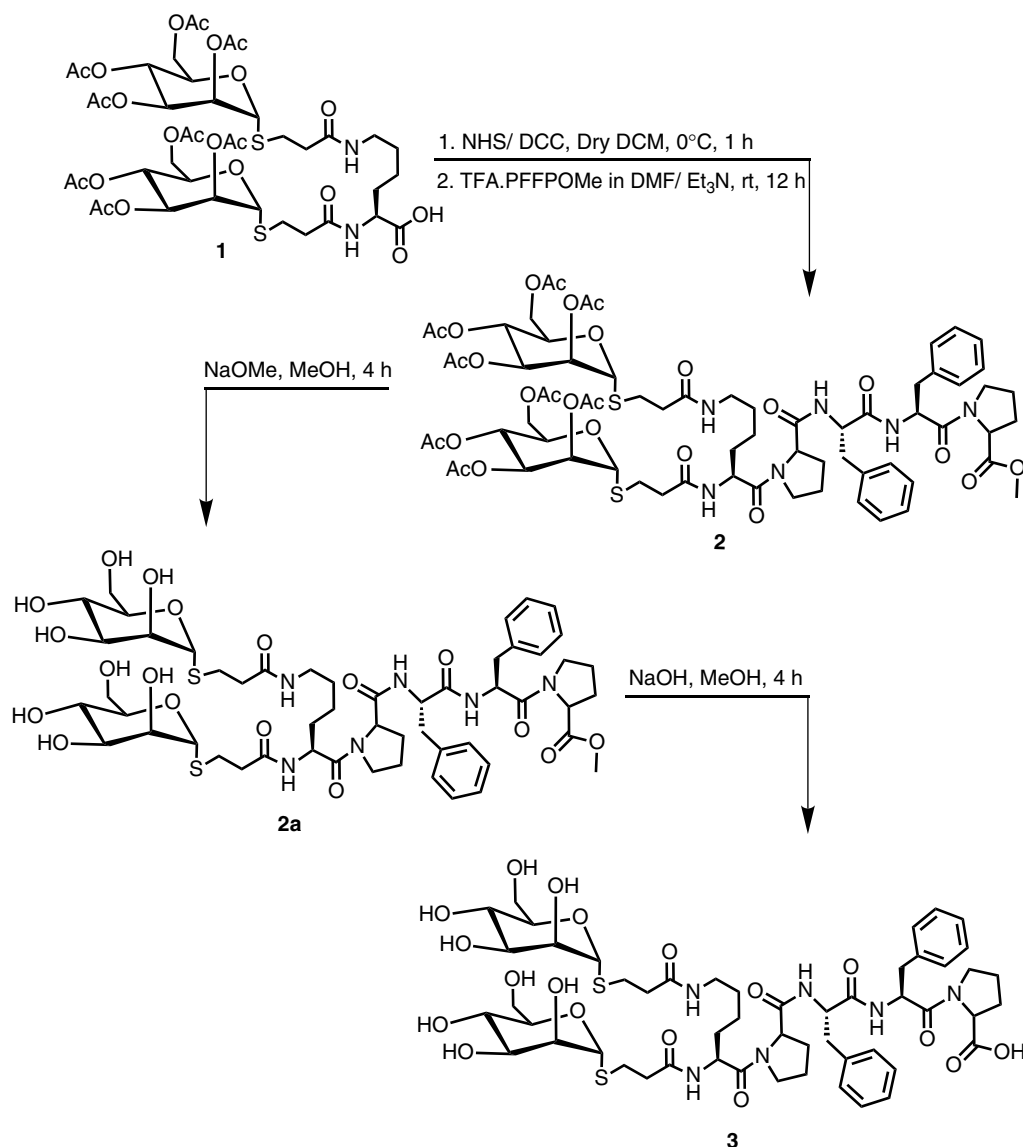


**Figure 1.** Synthetic scheme for compound **3**.

### Turbidimetric Assay

Time-dependent turbidimetric assay was performed in a quartz cell (1 cm × 1 cm). Aliquots of Con A solution (300 μl, 1.0 mg/ml) dissolved in HEPES buffer (10 mM, pH 7.4, containing CaCl<sub>2</sub> 1 mM, MnCl<sub>2</sub> 1 mM) were diluted with same HEPES buffer (1125 μl). Then a solution of **3** (1 mM, 10 μl) incubated for 12 h at 37 °C in water was added. UV spectra of mixture were recorded after every 2 min. The absorbance of mixture was monitored by scanning samples in range 250–600 nm and was recorded in UV visible spectrometer Varian Cary 100 Bio UV–Visible spectrophotometer.

### Agarose Gel Electrophoresis

Samples for gel electrophoresis were prepared by mixing 20 μl of pBR322 DNA (50 μg/ml) to **3** (180 μl, three different concentrations viz. 1, 0.5 and 0.1 mM were used) for 12 h at 37 °C. These samples were sonicated for 2 min in a sonicator from Entertech Pvt. Ltd. (200 W) under ice. Control samples were prepared by adding 20 μl of DNA to 180 μl of autoclaved water (DNA alone); 20 μl of DNA

added to 180 μl of 12 h aged solution of **3** and then sonicated for 2 min in a sonicator from Entertech Pvt. Ltd. (200 W) under ice. The samples were loaded onto 0.7% agarose gel containing ethidium bromide (1 μg/ml). Electrophoresis was carried out for 1 h at constant current (80 mA) in 0.5× TBE buffer (1.1 M Tris; 900 mM Borate; 25 mM EDTA; pH 8.3). Gels were imaged with a PC-interfaced Bio-Rad Gel Documentation System 2000.

### Acridine Orange Binding Assay with DNA

Compound **3** was dissolved in Acridine orange aqueous solution (10 μM) to a final concentration of 1.0 mM and incubated for 16 h at 37 °C. To this incubated solution (180 μl) was added 20 μl of DNA (50 μg/ml). One part of this aliquot was then sonicated for 2 min while other left as control. Greenish fluorescence inside sonicated sphere was visualized using fluorescent microscope (Leica DM2500M), provisioned with a fluorescence illuminator and a fluorescein filter (absorption 494 nm/emission 521 nm). For sonication studies, solution was sonicated for 2 min in a sonicator from Entertech Pvt. Ltd. (200 W) under ice.

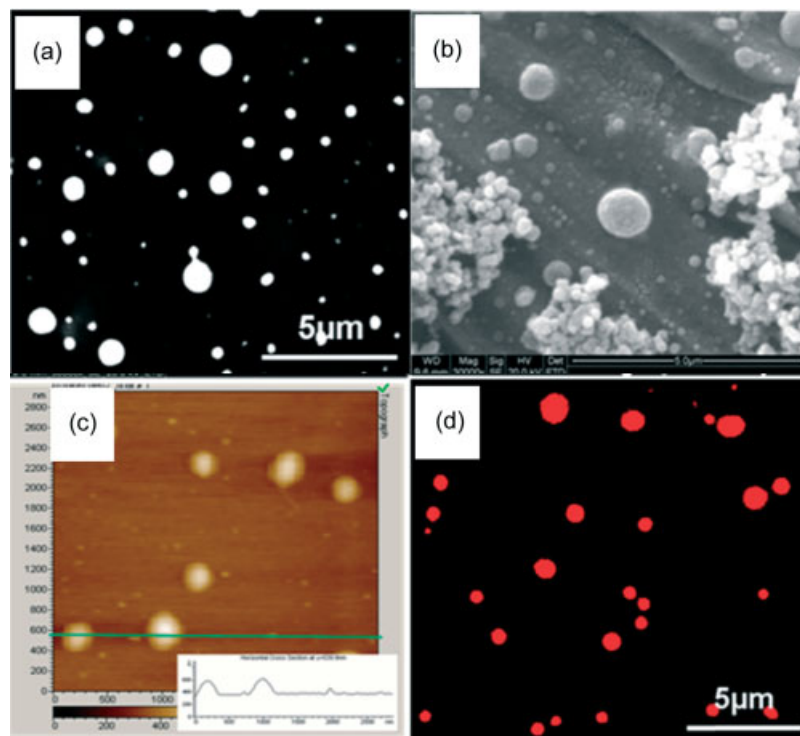


**Figure 2.** Microscopic images of spherical aggregates formed by self-assembly of **3** (1 mM, aqueous solution) after 12 h of incubation at 37 °C. (A) Optical micrograph of **3** on glass slide; (B) SEM micrograph of **3** on Cu stubs; (C) AFM image of spheres on mica; (D) Fluorescent micrograph showing intensely red spherical aggregates.

## Results and Discussion

Encouraged by our earlier studies where the tetrapeptide H-Pro-Phe-Phe-Pro–OH afforded spherical morphology in 50% aqueous methanol [21], we decided to conjugate this tetrapeptide with neoglycosylated lysine (**1**), with the aim of synthesizing water soluble conjugates to bring application of these soft structures in biological studies. The glycopeptide conjugate  $N^2, N^6$ -Bis[( $\alpha$ -D-mannopyranosyl)thio]propionyl]-Lys-Pro-Phe-Phe-Pro–OH (**3**) was synthesized as outlined in Figure 1 and its self-assembly properties were studied in aqueous medium.

Self-assembly of **3** was studied after aging the sample (1 mM) in aqueous solution at 37 °C for 12 h. Optical microscopic studies revealed the formation of spherical structures after 12 h of incubation in water (Figure 2(A)). SEM confirmed formation of spherical structures (Figure 2(B)). Further evidence was obtained from AFM experiments (Figure 2(C)). It was also possible to stain these structures with rhodamine B and fluorescence microscopy image once again afforded brightly stained spherical aggregates arising from the non-covalent ensemble of **3** (Figure 2(D)). This suggested that the gross morphology of self-assembly remained the same, while engineering a beneficial property of water solubility.

A closer inspection of the chemical structure of **3** reveals a surfactant-like, where hydrophobic peptide fragment could possibly be envisioned as a tail and the hydrophilic mannose residue may act as head group. As a result of the self-aggregation in aqueous solution, it is likely that the aromatic amino acid side chains get buried in the interior of the soft structure and the hydrophilic mannose residues will eventually decorate the exterior surface of spherical structures. A carbohydrate–lectin interaction assay was employed to test the projection of mannose

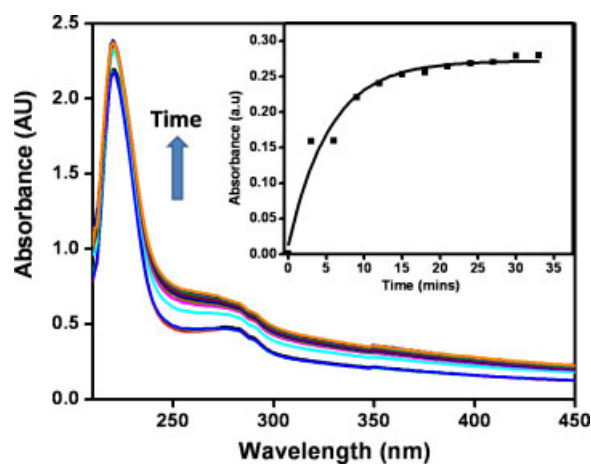


**Figure 3.** Interaction of **3** with Con A. UV visible spectrum of Con A with **3** at time intervals of 3 min shows turbidity (inset: turbidity with respect to time). This figure is available in colour online at [wileyonlinelibrary.com/journal/jpepsi](http://wileyonlinelibrary.com/journal/jpepsi).

units on the surface, based on the known mannose–Concanavalin A (Con A) interactions. The mannose–Con A interaction affords aggregation due to multivalent effect, thus enhancing turbidity of the solution [28–31]. Thus, a turbidimetric assay was performed to evaluate interaction of **3** with Con A and it leads to an increase in the absorbance at 400 nm as a function of time (Figure 3) (see supporting information). Such an observation suggests for the presence of mannose on the exterior of the spherical structures affording Con A aggregation, thus confirming the premise of exposed hydrophilic residues conferring water solubility to **3**.

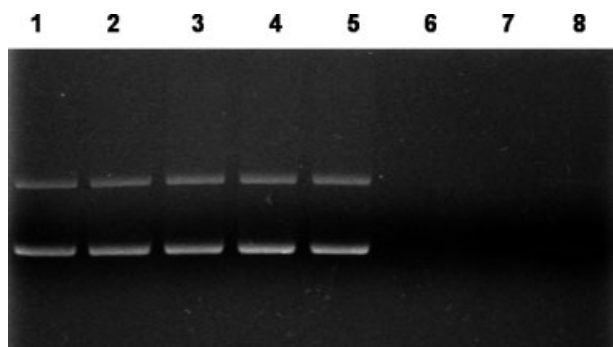


**Figure 4.** Gel of DNA with **3**: Lane 1: DNA alone; Lane 2, DNA coincubated with **3** (1 mM); Lane 3: DNA coincubated with **3** (0.5 mM); Lane 4: DNA coincubated with **3** (0.1 mM); Lane 5: DNA alone ultrasonicated for 2 mins; Lane 6, DNA coincubated with **3** (1 mM) ultrasonicated for 2 mins; Lane 7, DNA coincubated with **3** (0.5 mM) ultrasonicated for 2 mins; Lane 8, DNA coincubated with **3** (0.1 mM) ultrasonicated for 2 mins.

In our earlier study, we had reported that lysine conjugated with a biantennary mannose derivative (**1**) forms spherical structures that are hollow in nature and afford effective encapsulation of alkaline phosphatase enzyme, plasmid DNA and a GFP reporter gene, thereby illustrating their potential for confinement and delivery applications [19]. But these soft structures were not very robust and disrupted rather quickly when sonicated. It was thus of great interest to evaluate the stability of the soft structures of **3** for possible use as delivery vehicle for biologics, as the biological importance of glycoclusters is documented [32,33].

Using a standardized protocol, pBR322 was coincubated with **3** with an aim of encapsulating it within the confines of **3**, for gene delivery applications. Agarose gel electrophoresis of this mixture (Figure 4; lanes 2–4) revealed a band corresponding to pBR322 plasmid. The presence of DNA in the mixture suggested the lack of complexation/encapsulation of plasmid. Following our experience concerning disruption of soft structures with ultrasound, we decided to irradiate DNA–**3** mixture in an ultrasonic bath for 2 min, followed by electrophoresis. To our surprise, the band corresponding to pBR322 DNA disappeared (Figure 4; lanes 6–8). We surmise that these observations results from the gentle exposure of DNA–**3** complex to ultrasound resulting in complexation or encapsulation of DNA within the spherical aggregates of **3**. In a control experiment, DNA alone was ultrasonicated for 2 min to ensure that the disappearance of the plasmid band does not involve DNA degradation due to ultrasonication.

We resorted to Acridine orange dye binding assay to further ascertain the encapsulation of plasmid DNA in soft structures achieved from the self-assembly of **3**. Acridine orange is a nucleic acid selective fluorescent cationic dye and it interacts with DNA and RNA by intercalation or electrostatic attraction [34]. The appearance of green fluorescence on Acridine orange addition to DNA confirms the intercalation process. Ultrasonication of **3**, plasmid DNA and the dye in the same reaction mixture, afforded a bright green fluorescence contained within the spherical structures as observed by fluorescence microscopy (Figure 5(A) and (B)). Preformed spheres of **3** with added plasmid DNA, in the absence of ultrasound treatment, showed pale, diffused fluorescence when incubated with Acridine orange (Figure 5(C)). These experiments also suggest that controlled irradiation of ultrasound affords transient opening of pores/channels in the soft structures which enables DNA and Acridine orange to enter

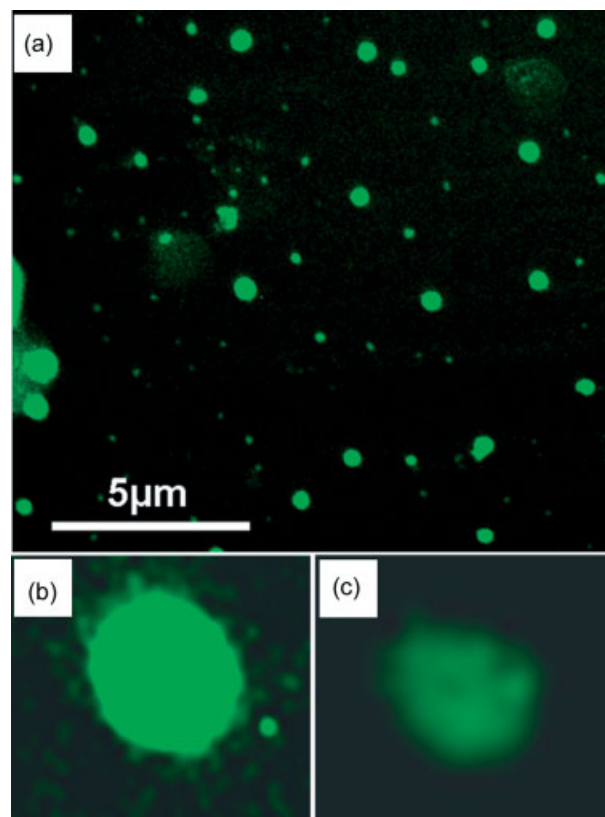


**Figure 5.** (A) Fluorescent micrograph of spheres of **3** which are ultrasonicated in presence of DNA showing green fluorescence due to binding of Acridine orange with DNA; (B) isolated sphere of **3** ultrasonicated in the presence of DNA; (C) Isolated spheres of **3** with added DNA, but not ultrasonicated.

the inner hollow compartment leading to intense, punctuated fluorescent response.

These results could be somewhat correlated to the concept of electroporation, where one capitalizes on the relatively weak nature of phospholipid bilayer hydrophobic/hydrophilic interactions and an impulse of mild current/voltage shock temporarily disrupts membrane, allowing polar molecules to pass through them [35,36]. This deformity in the lipid bilayer quickly dies out when the electrical impulse is discontinued and leaves the cell intact. This approach is used for transforming cell lines as it is not harmful to the cells. In a way, the entry of plasmid DNA in the soft spherical structures of **3**, upon mild ultrasound irradiation, resembles electroporation technique and offers an interesting alternate mechanism for transiently making the soft structures porous in nature.

## Conclusions

In conclusion, we have demonstrated that the *N,N*-bis-mannosyl-Lys-Pro-Phe-Phe-Pro-OH peptide derivative (**3**) exhibits self-association leading to the formation of spherical structures, in aqueous medium. The presence of multiple mannose residues on the surface will enable targeting of such structures to specialized cells such as dendritic cells, which are potent antigen-presenting cells that express several membrane lectins, including the mannose receptor. The soft structures offer DNA encapsulation upon sonication, which was ascertained by an increase in fluorescence

contained within spherical aggregates due to Acridine orange intercalation with encapsulated DNA. Thus, the self-assembling property of **3** and the possibility of loading cargo inside these structures suggest their possible use as delivery vehicles for specialized cells supporting multivalent mannose interactions.

### Acknowledgements

NG thanks IIT Kanpur for a pre-doctoral fellowship and SM thanks CSIR for a senior research fellowship. This work is supported by Department of Science and Technology, India (SV).

Special issue dedicated to E-MRS Symposium C "Peptide-based materials: from nanostructures to applications", 7-11 June 2010, Strasbourg, France.

### Supporting information

Supporting information may be found in the online version of this article.

### References

- 1 Yan X, Zhu P, Fei J, Li J. Self-assembly of peptide-inorganic hybrid spheres for adaptive encapsulation of guests. *Adv. Mater.* 2010; **22**: 1283–1287.
- 2 Mishra A, Panda JJ, Basu A, Chauhan VS. Nanovesicles based on self-assembly of conformationally constrained aromatic residue containing amphiphilic dipeptides. *Langmuir* 2008; **24**: 4571–4576.
- 3 Tanisaka H, Kizaka-Kondoh S, Makino A, Tanaka S, Hiraoka M, Kimura S. Near-infrared fluorescent labeled peptosome for application to cancer imaging. *Bioconj. Chem.* 2008; **19**: 109–117.
- 4 Guo B, Shi Z, Yao Y, Zhou Y, Yan D. Facile preparation of novel peptosomes through complex self-assembly of hyperbranched polyester and polypeptide. *Langmuir* 2009; **25**: 6622–6626.
- 5 Ha W, Meng X-W, Li Q, Fan M-M, Peng S-L, Ding L-S, Tian X, Zhang S, Li B-J. Self-assembly hollow nanosphere for enzyme encapsulation. *Soft Matter* 2010; **8**: 1405–1408.
- 6 Matsumoto S, Yamaguchi S, Wada A, Matsui T, Ikeda M, Hamachi I. Photo-responsive gel droplet as a nano- or pico-litre container comprising a supramolecular hydrogel. *Chem. Commun.* 2008; 1545–1547.
- 7 Iatrou H, Frielinghaus H, Hanski S, Ferderigos N, Ruokolainen J, Ikkala O, Richter D, Mays J, Hadjichristidis N. Architecturally induced multiresponsive vesicles from well-defined polypeptides. Formation of gene vehicles. *Biomacromolecules* 2007; **8**: 2173–2181.
- 8 Alarcon CDH, Pennadam S, Alexander C. Stimuli responsive polymers for biomedical applications. *Chem. Soc. Rev.* 2005; **34**: 276–285.
- 9 Yerushalmi R, Scherz A, van der Boom ME, Kraatz HB. Stimuli responsive materials: new avenues toward smart organic devices. *J. Mater. Chem.* 2005; **15**: 4480–4487.
- 10 Nath N, Chilkoti A. Creating "smart" surfaces using stimuli responsive polymers. *Adv. Mater.* 2002; **14**: 1243–1247.
- 11 Rijcken CJF, Soga O, Hennink WE, van Nostrum CF. Triggered destabilisation of polymeric micelles and vesicles by changing polymers polarity: an attractive tool for drug delivery. *J. Control. Release* 2007; **120**: 131–148.
- 12 Chécot F, Rodríguez-Hernández J, Gnanou Y, Lecommandoux S. pH-responsive micelles and vesicles nanocapsules based on polypeptide diblock copolymers. *Biomol. Eng.* 2007; **24**: 81–85.
- 13 Ozbas B, Kretsinger J, Rajagopal K, Schneider JP, Pochan DJ. Salt-triggered peptide folding and consequent self-assembly into hydrogels with tunable modulus. *Macromolecules* 2004; **37**: 7331–7337.
- 14 Napoli A, Valentini M, Tirelli N, Muller M, Hubbell JA. Oxidation-responsive polymeric vesicles. *Nat. Mater.* 2004; **3**: 183–189.
- 15 Bosques CJ, Imperiali B. Photolytic control of peptide self-assembly. *J. Am. Chem. Soc.* 2003; **125**: 7530–7531.
- 16 Murdan S. Electro-responsive drug delivery from hydrogels. *J. Control. Release* 2003; **92**: 1–17.
- 17 Collier JH, Hu BH, Ruberti JW, Zhang J, Shum P, Thompson DH, Messersmith PB. Thermally and photochemically triggered self-assembly of peptide hydrogels. *J. Am. Chem. Soc.* 2001; **123**: 9463–9464.
- 18 Park J, Rader LH, Thomas GB, Danoff EJ, English DS, DeShong P. Carbohydrate-functionalized cationic surfactant vesicles: preparation and lectin-binding studies. *Soft Matter* 2008; **4**: 1916–1921.
- 19 Gour N, Verma S. Bending of peptide nanotubes by focused electron and ion beams. *Soft Matter* 2009; **5**: 1789–1791.
- 20 Gour N, Purohit CS, Verma S, Puri R, Ganesh S. Mannosylated self-assembled structures for molecular confinement and gene delivery applications. *Biochem. Biophys. Res. Commun.* 2009; **378**: 503–506.
- 21 Joshi KB, Verma S. Sequence shuffle controls morphological consequences in a self-assembling tetrapeptide. *J. Peptide Sci.* 2008; **14**: 118–126.
- 22 Ghosh S, Reches M, Gazit E, Verma S. Bioinspired design of nanocages by self-assembling triskelion peptide elements. *Angew. Chem. Int. Ed.* 2007; **46**: 2002–2004.
- 23 Ghosh S, Verma S. Phased fiber growth in a peptide conjugate: aggregation and disaggregation studies. *J. Phys. Chem. B.* 2008; **11**: 3750–3757.
- 24 Ghosh S, Singh SK, Verma S. Self-assembly and potassium ion triggered disruption of peptide-based soft structures. *Chem. Commun.* 2007; 2296–2298.
- 25 Joshi KB, Verma S. Dityryptophan conjugation triggers conversion of biotin fibers into soft spherical structures. *Angew. Chem. Int. Ed.* 2008; **47**: 2860–2863.
- 26 Ghosh S, Verma S. Templated growth of hybrid structures at the peptide-peptide interface. *Chem. Eur. J.* 2008; **14**: 1415–1419.
- 27 Barman AK, Verma S. Sunlight mediated disruption of peptide-based soft structures decorated with gold nanoparticles. *Chem. Commun.* 2010; **46**: 6992–6994.
- 28 Kamiya N, Tominaga M, Sato S, Fujita M. Saccharide-coated m<sub>12</sub>l<sub>24</sub> molecular spheres that form aggregates by multi-interaction with proteins. *J. Am. Chem. Soc.* 2007; **129**: 3816–3817.
- 29 Fujimoto T, Shimizu C, Hayashida O, Aoyama Y. Ternary complexation involving protein. Molecular transport to saccharide-binding proteins using macrocyclic saccharide cluster as specific transporter. *J. Am. Chem. Soc.* 1998; **120**: 601–602.
- 30 Zanini D, Roy R. Synthesis of new  $\alpha$ -thiosialodendrimers and their binding properties to the sialic acid specific lectin from *Limax flavus*. *J. Am. Chem. Soc.* 1997; **119**: 2088–2095.
- 31 Aoi K, Itoh K, Okada M. Globular carbohydrate macromolecules "sugar balls". 1. Synthesis of novel sugar-persubstituted poly(amido amine) dendrimers. *Macromolecules* 1995; **28**: 5391–5393.
- 32 Mizuochi T, Spellman MW, Larkin M, Soloman J, Basa LJ, Feizi T. Carbohydrate structures of the human-immunodeficiency-virus (HIV) recombinant envelope glycoprotein gp120 produced in Chinese-hamster ovary cells. *Biochem. J.* 1988; **254**: 599–603.
- 33 Frison N, Taylor ME, Soilleux E, Bousser MT, Mayer R, Monsigny M, Drickamer K, Roche AC. Oligolysine-based oligosaccharide clusters: selective recognition and endocytosis by the mannose receptor and dendritic cell-specific intercellular adhesion molecule 3 (ICAM-3)-grabbing nonintegrin. *J. Biol. Chem.* 2003; **278**: 23922–23929.
- 34 Yamabe S. A spectrophotometric study on binding of acridine orange with DNA. *Mol. Pharmacol.* 1967; **3**: 556–560.
- 35 Xie TD, Sun L, Tsong TY. Study of mechanisms of electric field-induced DNA transfection. I. DNA entry by surface binding and diffusion through membrane pores. *Biophys. J.* 1990; **58**: 13–19.
- 36 Chang DC. Cell poration and cell fusion using an oscillating electric field. *Biophys. J.* 1989; **56**: 641–652.